J Mol Model (2010) 16:831–839
DOI 10.1007/s00894-009-0578-y

ORIGINAL PAPER

Excited state intramolecular proton transfer in 3-hydroxy flavone and 5-hydroxy flavone: A DFT based comparative study

Sankarlal Ash · Sankar Prasad De · Santanu Pyne · Ajay Misra

Received: 27 January 2009 / Accepted: 7 August 2009 / Published online: 18 September 2009

Abstract Potential energy (PE) curves for the intramolecular proton transfer in the ground (GSIPT) and excited (ESIPT) states of 3-hydroxy-flavone (3HF) and 5-hydroxy-flavone (5HF) were studied using DFT/B3LYP (6-31G (d,p)) and TD-DFT/B3LYP (6-31G (d,p)) level of theory respectively. Our calculations suggest the non-viability of ground state intramolecular proton transfer for both the compounds. Calculated PE curves of 3HF for the ground and excited singlet states proton transfer process explain its four state laser diagram. Excited states PE calculations support the ESIPT process to both 5HF and 3HF. The difference in ESIPT emission process of 3HF and 5HF have been explained in terms of HOMO and LUMO electron distribution of the enol and keto tautomer of these two compounds.

Keywords B3LYP · DFT · Excited state intramolecular proton transfer · 3-hydroxy-flavone · Potential energy

Introduction

Excited state intramolecular proton transfer (ESIPT) reactions are of great scientific and technological interest. Since its introduction, the photoinduced excited state intramolecular proton (or hydrogen) transfer reaction, which generally incorporate transfer of a hydroxyl (or amino) proton to the carbonyl oxygen (imine nitrogen) through a pre-existing intramolecular hydrogen bonding (IMHB) configuration, has received considerable attention, because it has led to a wide range of applications, such as laser dyes [1, 2], polymer stabilizer [3], raman filters [4], environmental probes in bio-molecules [5], etc. The main requirement of ESIPT reaction is that the molecule must have acid and basic groups and a strong intramolecular hydrogen bond between the two groups at the same time. The electronic excitation of the normal enol form (N) leads to the excited (N*) form, which in the course of photochemical reaction is transformed into a proton transferred keto tautomer (T*). 'T*' relaxes radiatively or non-radiatively to the metastable ground state keto tautomer 'T', which converts to 'N' state vis reverse proton transfer.

Since the original work of Weller [6] on the ESIPT of methyl salicylate (MS), a large number of experimental [7–14] and theoretical [15–21] studies on the ESIPT of a variety of systems have been reported. Flavonoids are a group of naturally occurring polyphenolic compounds ubiquitously found in fruits and vegetables [22–24]. The various classes of flavonoids differ in the level of oxidation of the 'C' ring (Scheme 1) of the basic benzo-γ-pyrone structure. Common family members of flavonoids include flavones, flavanes, flavonols, catechins and anthocyanidins. Flavonols are flavonoids of particular importance because they have been found to possess antioxidant and free radical scavenging activity in foods [25]. Flavonols [3HF,5HF] and their derivatives usually exhibit two strongly separated bands in their fluorescence spectrum due to ESIPT reaction, leading to two excited forms, the normal N* and the tautomer T* ones. Their positions and relative intensities depend on several parameters of the medium. Due to this unique phenomenon many flavonol derivatives were shown to be very effective probes in the analysis of the structure of micelles [26–28] and phospholipid vesicles [29–31], as well as in the

Electronic supplementary material The online version of this article (doi:10.1007/s00894-009-0578-y) contains supplementary material, which is available to authorized users.

S. Ash · S. P. De · S. Pyne · A. Misra (✉)
Department of Chemistry and Chemical Technology,
Vidyasagar University,
Midnapore 721 102 W.B, India
e-mail: ajaymsr@yahoo.co.in

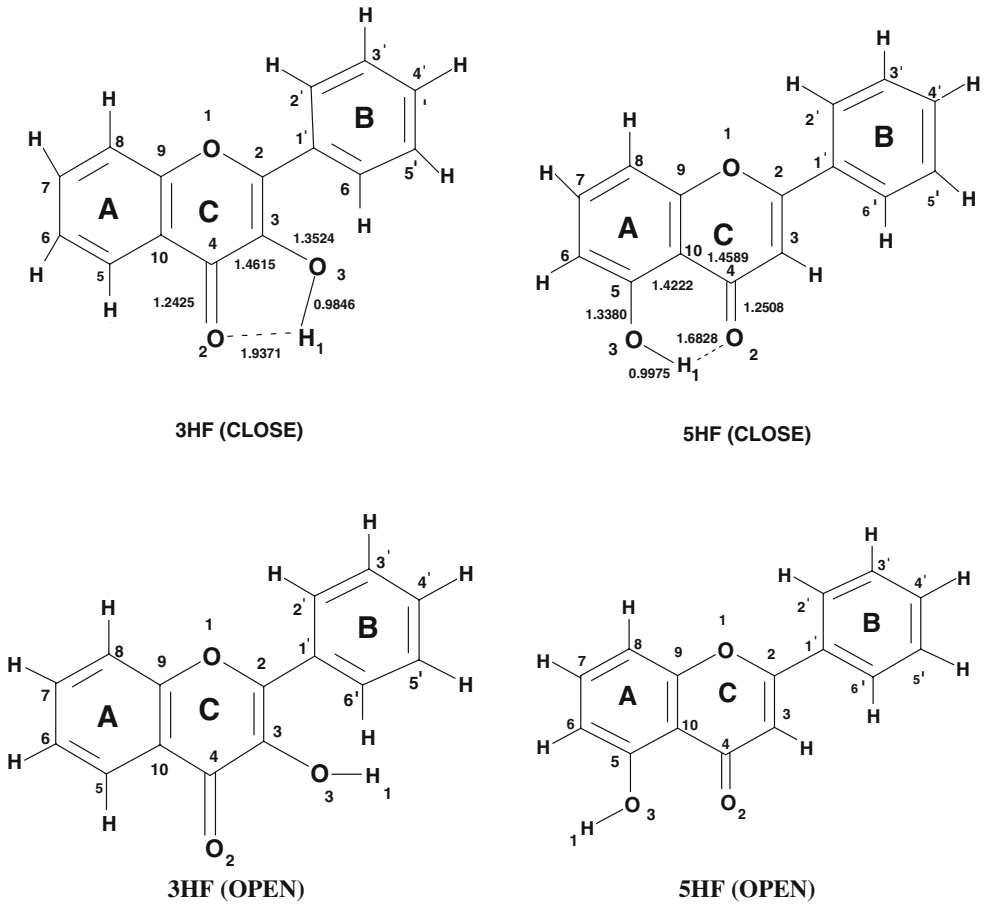

Scheme 1 Optimized intramolecular hydrogen bonded (close) and non-hydrogen bonded (open) structure of 3-hydroxy flavone (3HF) and 5-hydroxy flavone (5HF)

fluorescence recognition of cations of different radii [32, 33]. Among the flavonol class, 3HF has been widely studied because of its green fluorescence, which was ascribed to the proton transfer fluorescence [34]. The present understanding of the photophysics of 3HF is due to the efforts of several groups [8]. The proton transfer process in 3HF was discovered by Sengupta and Kasha [34] who assigned the previously observed dual fluorescence bands of 3HF to a normal N* isomer (λ_{em}=408 nm.) and T* tautomer (λ_{em}= 530 nm.). 3HF was the first intramolecular proton transfer laser dye reported in the literature [34, 35] and has been extensively utilized as fluorescence probe in bio-molecules [36–39]. On the other hand 5HF was once recognized as a completely 'non-luminescent' molecule. Recently, the resolution of fluorescence spectrum of 5HF has been achieved by using laser induced fluorescence technique. With the help of laser induced fluorescence study Chou et al. [40] showed dual emission band for 5HF maximized at 420 nm and 700 nm respectively. The 420 nm band is normal emission band and the 700 nm band is assigned as the tautomeric emission band arises due to excited states intramolecular proton transfer in 5HF. It is now well established that both 3HF and 5HF show dual emission band. However unlike 3HF, it took quite a long time, till the invention of laser induced fluorescence technique, to establish the dual emission band of 5HF.

Though the experimental work on the ESIPT of flavonols were initiated by Sengupta et al. and later on by the other research groups [41–43] in the early 1980s, theoretical investigations to understand the inner intricacies involved in the ESIPT process of 3HF & 5HF has been started very recently [44–46]. In a recent communication [47], we investigated the ESIPT process in 5HF in terms of its ground and excited states potential energy surface as well as the HOMO, LUMO electron density of the intramolecular hydrogen bonding ring system. Now the wide differences in emission properties of 3HF and 5HF motivate us to carry out the present extensive quantum chemical calculations to get some insight in terms of their electronic structure.

Hybrid HF/DFT methods have been proposed as reliable tools for computing static and dynamic properties of hydrogen-bonded systems [48–50]. One such method, B3LYP [52], nicely predicts the available experimental data, as well as the results obtained with the highest post-HF method [53]. In view of its wide spread success for the calculation of large

molecules [50, 51], we decided to choose density functional approach for the present comparative study on the excited state intramolecular proton transfer process in 3HF and 5HF. Our PES calculations nicely explain the four state laser diagrams for 3HF and also the low emission yield of 5HF. The wide difference in ESIPT process between these two compounds has also been explained in terms of HOMO, LUMO electron denotes of the IMHB ring system.

Theoretical calculations

All ab initio calculations reported in this paper were carried out using the Gaussian 03 suite programs [54]. We compared the results for a number of method and basis sets and found that the DFT based calculations using hybrid functional (B3LYP) with 6-31G(d,p) basis set to be the optimal one in terms of price-performance ratio for carrying out present electronic structure calculations within our limited computational resource. Analytic vibrational frequency computations at the optimized structure were done to confirm the optimized structure to be an energy minimum or a transition structure.

Strength of the intramolecular hydrogen bond (IMHB) of 3HF and 5HF was evaluated as the difference between energy of the fully optimized structure of the non-hydrogen bonded open form and energy of the N-tautomer, i.e. close form.

Methodology for PES calculations

Ground state optimized structure of both 3HF and 5HF shows that the enol tautomer ('N') is the stable form having strong intramolecular hydrogen bond (Scheme 1). Bond length, bond angle and dihedral angle data of both 3HF and 5HF obtained by HF/6-31G(d), DFT-B3LYP/6-31G(d), DFT-B3LYP/6-31G(d,p) level of theory along with those of X-ray crystal structure data are listed in supplementary data section. Comparison of X-ray crystal structure data with those calculated shows that the values obtained from DFT-B3LYP/6-31G (d,p) level of theory is closer to the experimental values. So we believe DFT-B3LYP/6-31G (d, p) will be the best among the three listed theoretical methods for the potential energy calculation of 3HF and 5HF.

The conversion from 'N' to 'T' in the ground electronic state can be thought of as arising due to the transfer of proton from O(3) to O(2) with simultaneous redistribution of electron density within the five-member hydrogen bonded ring. Some authors [55] have considered the O(3)-O(2) distance as fixed and varied the O(3)-H(1) bond distance to get an idea about the potential energy curve for both ground and excited states intramolecular proton transfer processes. A plot of O(3)-O(2) distance as a function of $r_{O(3)\text{-}H(1)}$ of 3HF as shown in Fig. 1 revels that as the proton shifted from O(3) to O(2), the O(3)-O(2) distance changes significantly. At smaller O(3)-H(1)

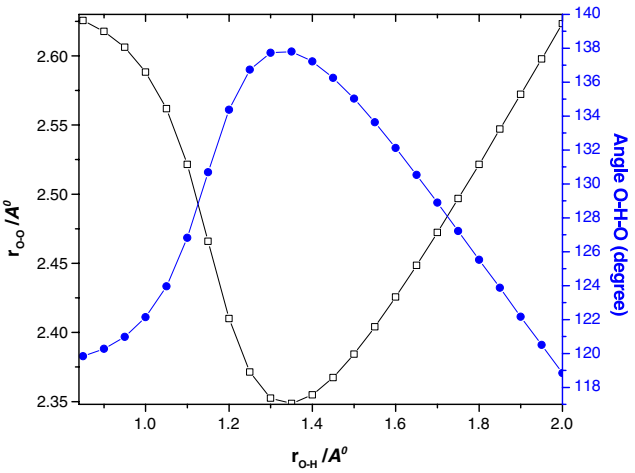

Fig. 1 Variation of O(3)-O(2) distance and O(3)-H(1)-O(2) angle of 3HF with $r_{O(3)\text{-}H(1)}$ as obtained from DFT-B3LYP(6-31G(d,p)) level of theory

distance it decreases slowly. In the close vicinity of a stable O(3)-H(1) distance (~1.00A^0), the O(3)-O(2) distance falls sharply and with the further increase of O(3)-H(1) distance, it decreases, passes through a minima (at $r_{O(3)\text{-}H(1)}$=1.35 A^0) and then enlarges to a distance comparable to that in the 'T' form. Figure 1 also shows variation of O (3)-H (1)-O (2) angle as a function of $r_{O(3)\text{-}H(1)}$ distance. At smaller O (3)-H (1) distance, it increases slowly. The O (3)-H(1)-O(2) angle increases sharply in the near vicinity of the stable O(3)-H(1) distance. Then increases with the increase of $r_{O(3)\text{-}H(1)}$ distance, reaches maximum (at $r_{O(3)\text{-}H(1)}$=1.35A^0) and then shows a sudden fall with the further increases of $r_{O(3)\text{-}H(1)}$ distance. We obtain similar variation of $r_{O(3)\text{-}O(2)}$ and O(3)-H (1)-O(2) angle with $r_{O(3)\text{-}H(1)}$ in case of 5HF. Therefore it is obvious that by freezing the geometry or by fixing the O(3)-O(2) distance at a particular values, one ends up introducing artificial constraints on the system and hence a barrier for the enol (N) to keto (T) conversion.

In this article we use the "distinguished co-ordinate" approach as proposed by Sobolewski et al. [56], where O (3)-H (1) bond distance is varied and the rest of the structural parameters are allowed to relax for each choice of $r_{O(3)\text{-}H(1)}$. Maheswari et al. [57] did an extensive theoretical study on salicylic acid and showed that the variation of O(3)-H(1) bond length can be used as reaction co-ordinate in order to get some idea about the PE curve for the ground as well as excited state proton transfer processes. Catalan et al. [48] also used the similar reaction co-ordinate ($r_{O(3)\text{-}H(1)}$) for the ESIPT processes of some naphthalene derivatives. In recent communications we showed that the use of $r_{O(3)\text{-}H(1)}$ distance as reaction co-ordinate can explain nicely both the ground and excited states potential energy surface and hence the ESIPT processes in 1 hydroxy- 2-naphthaldehyde, 2-hydroxy-3-naphthaldehyde [58], 5-hydroxyflavone [47] and O-hydroxy-benzaldehyde [59].

Ground state intramolecular proton transfer (GSIPT) curves were calculated with energies of the B3LYP/6-31G (d,p) fully optimized structures at fixed O-H distances over the 0.85 – 2.0 A^0 range. Information on the ESIPT curve was obtained by calculating the Franck-Condon (FC) transition energies for the DFT (B3LYP)/6-31G (d,p) ground state structures at the TD-DFT (B3LYP)/6-31G (d,p) level of theory. The Franck-Condon (FC) curves for the proton transfer processes were obtained by adding the TD-DFT (B3LYP)/6-31G (d,p) excitation energies to the corresponding GSIPT curves. Again the agreement of TD-DFT (B3LYP)/6-31G (d,p) result with absorption wavelength (λ_{max}) helps us to the TD-DFT (B3LYP) level of theory for excited states PES calculations.

Results and discussion

Ground state optimized structure of 3HF and 5HF shows that the enol form ('N') is the most stable form due to the presence of strong intramolecular hydrogen bonds (Scheme 1) in both of the compounds.

Comparison of IMHB

In order to get some idea about the relative strength of IMHB in 3HF and 5HF, we compared the C = O and O-H stretching frequencies of these two compounds with some model compounds like flavone, 3-hydroxy-2-phenyl-4-H-chromene, 5-hydroxy-2-phenyl-4-H-chromene (Table 1). We used B3LYP/6-31G (d,p) level of theory for calculation of frequencies and 0.9613 was used as scale factor for frequencies as given in ref. [54]. Table 1 shows that our methodology for calculation of vibrational frequencies works nicely, since our calculated C = O and O-H stretching frequencies agree well with the available experimental data (Table 1). It is reasonable to infer from both the experimental as well as theoretical calculations that the position of O-H absorption in 3-hydroxy-2-phenyl-4-H-chromene shows large red shift, compared to O-H absorption in 3HF where strong IMHB is present. Greater red shift of the band positions from its mono-substituted compound, i.e. larger values of $\Delta\nu_{OH}$ and $\Delta\nu_{C=O}$ are taken as evidence for stronger IMHB [60]. Now both the experimental and theoretical data of $\Delta\nu_{OH}$ and $\Delta\nu_{C=O}$ in Table 1 suggests that strong IMHB are present within 5HF. A comparison of $\Delta\nu_{OH}$ (463 cm^{-1} for 3HF and 633 cm^{-1} for 5HF) and $\Delta\nu_{C=O}$ (35 cm^{-1} for 3HF and 27 cm^{-1} for 5HF) for 3HF and 5HF are shown in Table 1 and it illustrates that IMHB in 3HF is much weaker than 5HF.

A comparison of ground state intramolecular hydrogen bond strength for both 3HF and 5HF are also calculated, by rotating the phenolic -OH group out of the hydrogen bonded conformation and computing the difference in energy between the closed and open form for 3HF and 5HF (Fig. 2). The calculated IMHB strength for 3HF and 5HF are found to be 10.48 kcal mol^{-1} and 15.00 kcal mol^{-1} respectively. Figure 2 also shows that the barrier for phenolic -OH rotation and it is found to be 11.80 kcal mol^{-1} in 3HF and 18.90 kcal mol^{-1} in 5HF. The intramolecular hydrogen bond forms five and six member ring systems in 3HF and 5HF respectively. We believe, due to higher ring strain in the five member ring system than its six member counterpart, the relative strength of IMHB in 3HF will be less than 5HF.

Ground and excited state potential energy curve of 3HF

Potential energy surface (PES) along the proton transfer co-ordinate, i.e. $r_{O(3)\text{-}H(1)}$ for both the ground and the first excited singlet state of 3HF are shown in Fig. 3 . Ground state calculation shows a minimum in the PE curve at $r_{O(3)\text{-}H(1)}$ distance near about 1.00 A^0 and this is due to the 'N' tautomeric form of 3HF. Ground state potential energy curve increases steadily as the $r_{O(3)\text{-}H(1)}$ distance increases from 1.00 A^0 – 1.30 A^0 and from 1.40 A^0–2.00 A^0 curve (S_0') shows a wide minimum with a very small depth around 1.70A^0 where the $r_{O(2)\text{-}H(1)}$ distance is 1.01 A^0. Franck-

Table 1 Theoretical and experimental carbonyl and hydroxyl stretching frequency values of 3HF, 5HF and some model compounds

Compounds	C = O stretching frequencies (in cm^{-1})		O-H stretching frequencies (in cm^{-1})		$\Delta\nu_{C=O}$		$\Delta\nu_{O\text{-}H}$	
	Theo.	Exp.[a]	Theo.	Exp.[a]	Theo.	Exp.[a]	Theo.	Exp.[a]
3HF	1641	1652	3185	3320	35	17		
5HF	1649	1660	3053	2935	27	09		
Flavone	1676	1669						
2-phenyl-3- hydroxy-4H- chromene [b]			3648				463	
2-phenyl-5- hydroxy-4H- chromene [b]			3686				633	

[a] Petroski et al., J. Phys. Chem. A 106(2002)11714

[b] Experimental results are not available

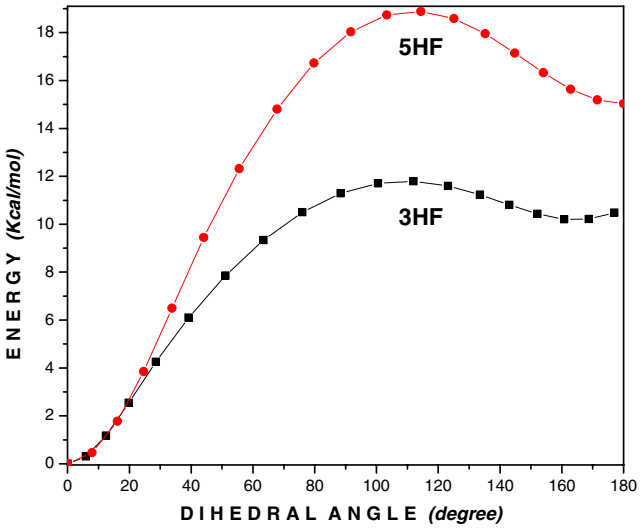

Fig. 2 Energetics of the transformation from IMHB from (N) to the non-hydrogen bonded form (hydroxyl group rotated from 0 to 180^0) of 3HF and 5HF. For each value of dihedral angle H (1)-O (3)-C (3)-C (4). and H (1)-O (3)-C (5)-C (10). respectively, the geometry has been optimized using the DFT-B3LYP/6-31G (d,p) level of theory

Condon (FC) potential energy curve for the S_1 and S_1' state shows two minima, one at $r_{O(3)\text{-}H(1)}$=1.00 A^0 and the other which is much lower in energy at about $r_{O(3)\text{-}H(1)}$=1.75 A^0. The former is due to the excited enol form (N*) and the latter minima is due to excited keto tautomer (T*). Wide minima with small depth around the keto tautomer position of GSIPT curve (S_0') and small energy gap between $S_0'$and S_1' curve ($r_{O(3)\text{-}H(1)}$=1.70 A^0) suggest that the keto tautomer emission will be broad, structured less and red shifted. Relative ordering of states of S_0, S_0', S_1' and S_1 as shown in Fig. 3 are the same as that schematically proposed by Khan et al. [35] while explaining the lasing action of 3HF. Small proton transfer barrier and exothermal nature of the PES of S_1 state will populate the S_1'state. Again the low barrier and downhill potential while going from S_0' to S_0 state will depopulate the S_0' state through back proton transfer. The uneven rate of the excited state proton transfer and ground state back proton transfer will result in inversion of population between $S_1'$and $S_0'$and hence it can show lasing action while decay radiatively from $S_1'$to S_0', i.e. during keto tautomer emission.

Compared to our previous studies on some hydroxy naphthaldehyde [58] and 5-hydroxyflavone [47], where the ground state potential energy surface for the keto tautomer (S_0') are either flat or repulsive in nature, 3HF shows a little depth in its S_0' state. Sengupta et al. [34] observed a large stokes shifted, emission band of 3HF in 2-methyl butane maximized at ~520 nm along with the normal emission band at 410 nm. The red shifted emission is due to excited keto tautomer (T*) resulted from ESIPT along the proton transfer co-ordinate. Experimental investigations of Sengupta et al. showed that λ_{max} of 3HF in 2-methyl butane is ~335 nm. On the other hand, our calculated λ_{max} in the gas phase is ~347 nm and this is in good agreement with their experimental findings.

Free energy calculations for the enol ⇆ keto equilibria of 3HF give a positive value of free energy change (ΔG= 11.39 kcal mol^{-1}) and the calculated equilibrium constant is ~5×10^{-9}. On the basis of the equilibrium constant, the population ratio in the gas phase for enol vs. keto form in the ground state is 0.2×10^9: 1. This clearly explains that proton transfer in the ground state is not thermodynamically favourable in 3HF.

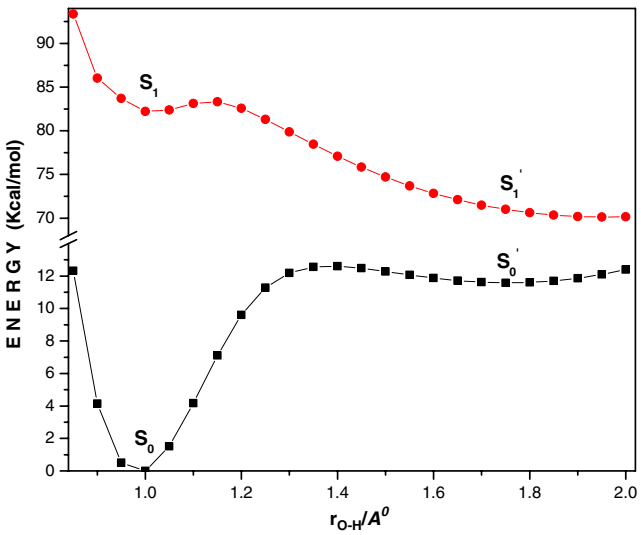

Fig. 3 GSIPT curve (S_0, S_0') and ESIPT Franck-Condon curve (S_1, S_1') of 3HF as obtained from DFT-B3LYP/6-31G (d,p) and TD-DFT-B3LYP/6-31G (d,p) level of theory

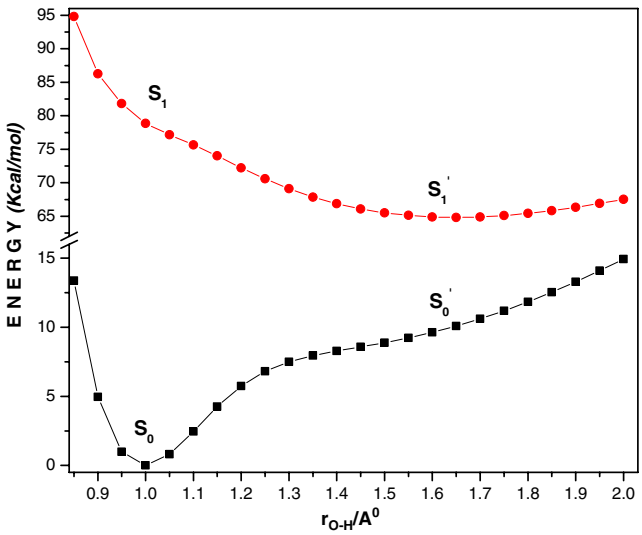

Fig. 4 GSIPT curve (S_0, S_0') and ESIPT Franck-Condon curve (S_1, S_1') of 5HF as obtained from DFT-B3LYP/6-31G (d,p) and TD-DFT-B3LYP/6-31G (d,p) level of theory

Ground and excited state potential energy curve of 5HF

Figure 4 shows the variation of potential energy along the proton transfer co-ordinate for both the ground and the first excited singlet state of 5HF. Ground state PE curve shows a minimum at a distance ~1.00 A^0 and this is due to the 'N' form of 5HF. Surprisingly, there is no shallow minima for the 'T' form, rather the ground state potential energy curve increases steadily as the $r_{O(3)-H(1)}$ distance increases from 1 to 2 A^0. FC potential energy curve for the S_1 state shows a global minimal at $r_{O(3)-H(1)}$=1.60 A^0 and a local minima at $r_{O(3)-H(1)}$=1.00 A^0. The former is due to the excited keto form (T*) and the latter is due to the locally excited enol tautomer (N*). Repulsive nature of the GSIPT curve and the energy gap between S_0' and S_1' predicts that the keto tautomer emission will be broad, structureless and red shifted. In their laser induced fluorescence measurements, Chou et al. [36] observed a large stokes shifted, extremely weak broad emission band of 5HF maximized at ~700 nm for the keto tautomer resulted from ESIPT.

In a previous communication [47] we showed that the ground state proton transfer process in 5HF is thermodynamically unfavourable. We also showed that our present adapted methodology for the calculation of ESIPT showed good agreement between the calculated and experimental λ_{max} values.

Comparison of IMHB and ESIPT of 3HF and 5HF:

Both the compound 3HF and 5HF contain two chromophore -OH and -C = O, but they differ only on the relative position of the -OH group. Our calculation suggests that for both of these molecules the 'N' form is the most stable in their ground state. Strength of IMHB is nearly 4.5 kcal mol-1 more in 5HF than 3HF.

Figure 4 shows that the excited singlet, i.e. $^1(\pi\pi^*)$ state potential energy curve of 5HF has a minimum at the equilibrium distance of the N-tautomer and a wide minimum with a very low energy near the keto tautomer position. The figure also shows that the barrier between of N*-tautomer and T*-tautomer is very small. If the proton transfer process or any other non-radiative deactivation channel is quite fast compared to the lifetime of excited N-tautomer, as is observed by Chou et al. [40] for 5HF, it will be very difficult to observe the emission from N-tautomer. On the other hand, due to the faster formation rate, population of T-tautomer will be enough to observe emission. Thus in order to observe emission from N* of 5HF one has to increase the

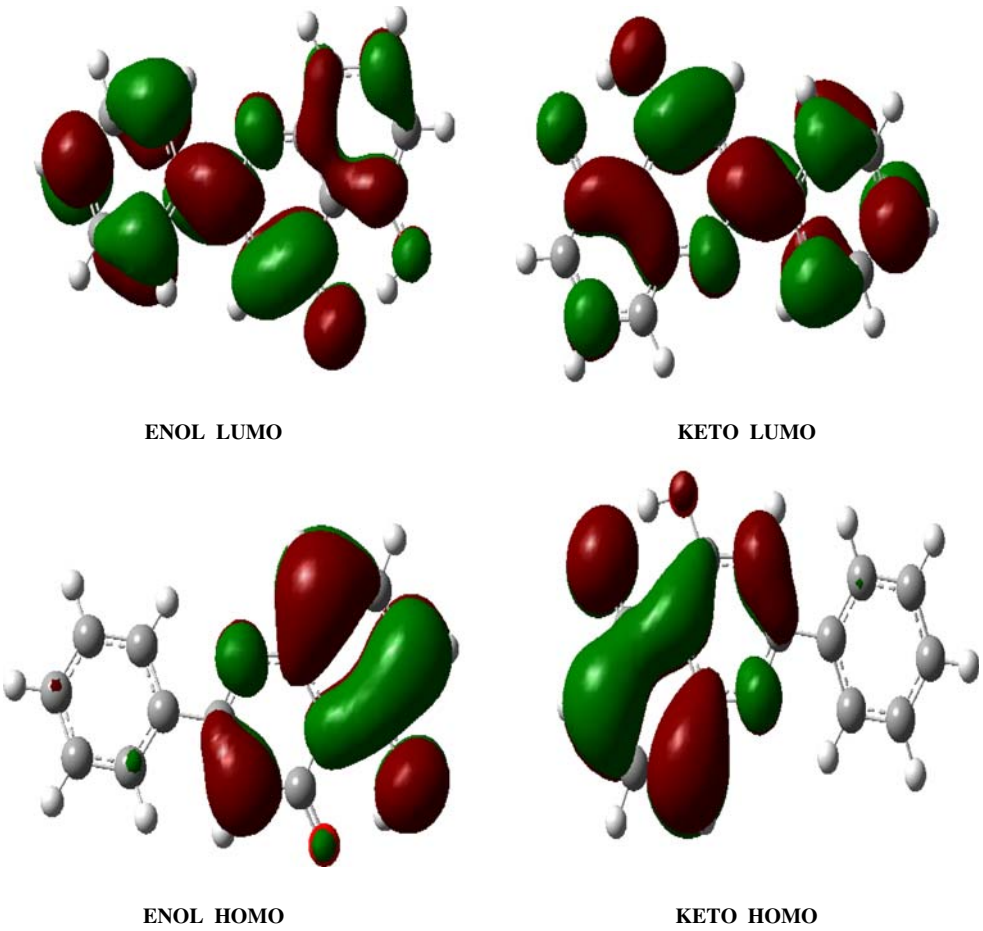

Fig. 5 HOMO and LUMO of 5HF (enol and keto) as obtained with DFT-B3LYP/6-31G (d,p) level of theory

concentration of N* with the help of some intense source of radiation, e.g. laser radiation, and also the detection system should be highly sensitive. The $^1(\pi\pi^*)$ potential energy curve of 3HF exhibits two minima with a comparatively higher energy barrier between N* and T* tautomers. Due to this high barrier, both the N* and T* species can have considerable population and thus giving dual emission upon excitation in the $^1(\pi\pi^*)$ state.

A detailed analysis of the electron distribution of HOMO and LUMO of these two compounds can provide some light on the ground and excited states proton transfer processes. Both HOMO and LUMO are of π type, but their phases are quite different in 3HF and 5HF. HOMO of the 5HF enol form (Fig. 5) shows that intramolecular hydrogen bonded (IMHB) ring system is primarily of bonding character over the O(3)H (1) and C(5)C(10) atoms, where as C(4) is *anti*-bonding character. Both the hydroxyl oxygen (O (3)) and carbonyl oxygen (O (2)) have bonding character, with a larger electron distribution over the hydroxyl oxygen (O (3)). Electron distribution of HOMO of keto tautomer around IMHB ring shows *anti*-bonding character over the H(1)O(3), O(3)C(5) and C(4)O(2) atoms and bonding character over the C(5)C (10)C(4) atoms. Again compared to HOMO of enol form, HOMO of keto shows much larger electron distribution on O (3). HOMO electron distribution for both the enol and keto form shows less electron distribution over the phenyl ring. Whereas HOMO orbitals on the IMHB ring system of 3HF (Fig. 6) is primarily of bonding in nature over the C(3)C(4), O(2) and O(3)-H(1) atoms, where as C(4)O(2) and C(3)O(3) shows *anti*-bonding character. Both the hydroxyl oxygen (O (3)) and carbonyl oxygen (O (2)) have bonding character, with a little larger electron distribution over the hydroxyl oxygen (O (3)). Analysis of the HOMO electron distribution (Fig. 6) after the ground state proton transfer still shows larger π-electron distribution on O(3) and also an increase of electron distribution over the C(3)C(4) bond. Electron distribution of HOMO of keto tautomer around the IMHB ring shows *anti*-bonding character over the same atoms, i.e. C(3)O(3), C(4)O(2) as in the normal form and bonding character over the C(3)C(4), O(3) and O(2) atoms. HOMO electron distribution of the ground state proton transfer form of 3HF (Fig. 6) shows less electron distribution on hydroxyl oxygen and lower delocalization than that of 5HF. Thus the lower conjugation through the IMHB ring in 3HF weakens its IMHB strength. Again the less effective electron transfer along the proton transfer co-ordinate makes the GSIPT

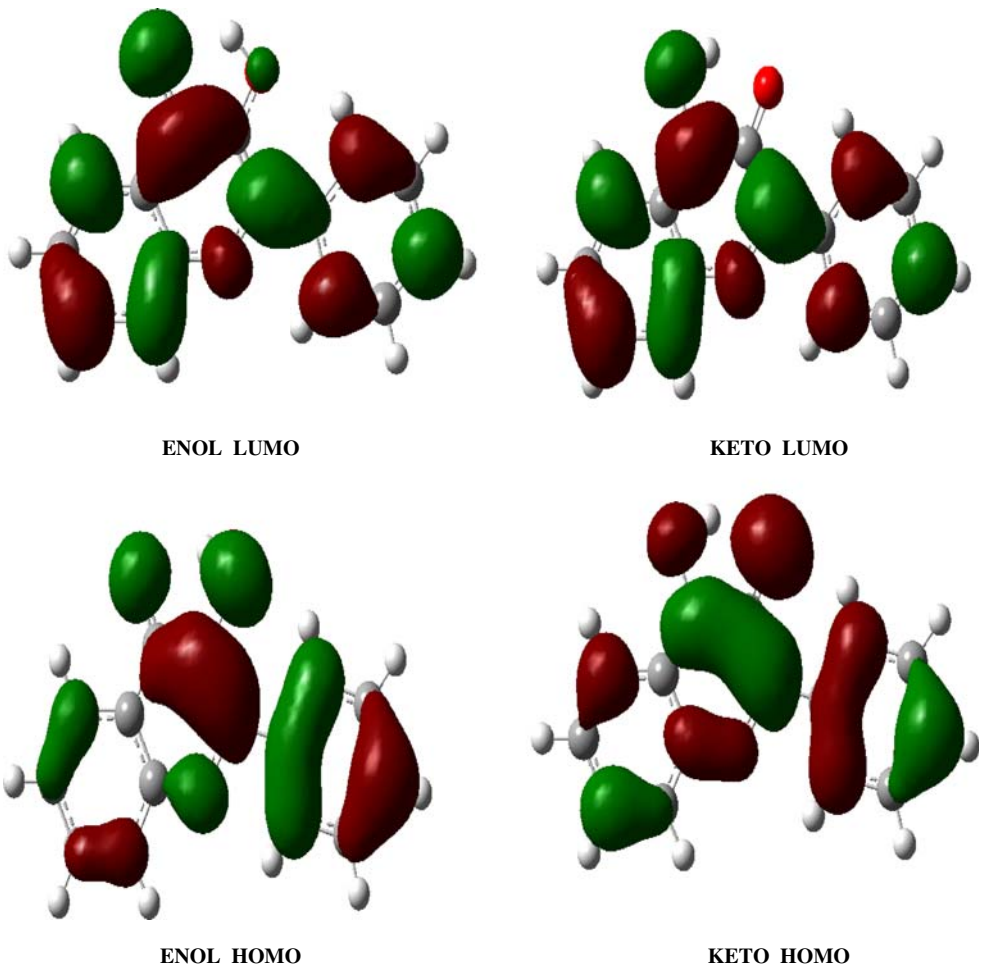

Fig. 6 HOMO and LUMO of 3HF (enol and keto) as obtained with DFT-B3LYP/6-31G (d,p) level of theory

process less probable. The opposite effect was found for 5HF, thereby strengthening the IMHB ring system and stabilization of the GSIPT potential energy curves with respect to 3HF. Nevertheless, this stabilization is not sufficient for producing a GSIPT process. Because for both the compounds analysis of electron distribution of HOMO for enol tautomer(N) predicts O(3) has slightly higher bonding character than O(2). Again, HOMO electron distribution of keto tautomer(T) suggest much greater bonding character of O(3) than O(2) and hence transfer of proton from O(3) to O(2) in the ground state is quite impossible.

For both 5HF (Fig. 5) and 3HF (Fig. 6) LUMO is π* in nature. If we look into the electronic charge distribution of LUMO for 5HF (Fig. 5) within IMHB ring of N-tautomer, C(5)C(10) position have bonding character, whereas C(10)C(4), C(4)O(2) and C(3)C(5) have *anti*-bonding character. LUMO of the enol tautomer possess high electron distribution on O (2). Again our calculation of electron distribution over the proton transfer co-ordinate in the excited states (i.e. LUMO electron distribution) shows that there is a shift of π-electron distribution from O (3) to O (2). In case of 3HF electronic charge distribution of LUMO (Fig. 6) within IMHB ring of N-tautomer, C(3)C(4) position have bonding character, whereas O(3)C(3), C(4)O(2) have *anti*-bonding character. LUMO of the enol form possess high electron distribution on the O (2) atom (Fig. 6). After tautomerization, the LUMO of the keto tautomer(Fig. 6) still shows high electron distribution on the O(2) atom and much lower electron distribution on the O(3) atom. Thus it favours the transfer of a proton from O (3) to O (2) in the excited state. However, in the case of LUMO of the keto tautomer of 5HF (Fig. 5.) both O (2) and O (3) have almost similar electron distribution. So ESIPT process in 5HF is less favourable compared to 3HF.

Conclusions

Our computational study suggests that the relative position of the -OH and C = O group in 3HF & 5HF determine the strength of intramolecular hydrogen bond and the nature of ESIPT emission. Ground state IMHB strength in 5HF is more compared to 3HF. Free energy, HOMO electron distribution and also ground state PE calculation for both 3HF and 5HF support the non-viability of GSIPT processes. On the other hand, excited state potential energy and LUMO electron distribution calculations support the ESIPT for both 3HF and 5HF. The nature of the ground and excited state potential energy curve nicely explains the red shifted broad structure less emission band of 5HF and also a large stokes shifted and broad ESIPT band of 3HF. Again for both of these compounds the energy gap between the excited singlet and ground singlet states is quite small compared to our previously studied compounds [47, 58, 59]. According to the energy gap law, non-radiative transition from T* will be faster and there will be a competition between the radiative and non-radiative transition. We believe, due to the faster formation rate of 'T*' (as it is obvious from the exothermal nature of the excited state potential energy surface) and also the presence of other faster non-radiative deactivation channel from 'N*' as well as 'T*', quantum yield of emission from both the excited enol ('N*) and keto ('T*') tautomer of 3HF would be very low. Relative ordering of energy states (S_0, S_0', S_1', S_1) and exothermal nature of the potential curve from $S_1 \rightarrow S_1'$ and $S_0' \rightarrow S_0$ nicely explains the development of inversion of population between S_1' and S_0' state and the use of 3HF as proton transfer laser dye. Analysis of the LUMO electron distribution suggests that ESIPT is more favourable in 3HF than 5HF.

Acknowledgments We gratefully acknowledge the financial support received from Department of Science & Technology (ref. No. SR/FTP/PS-60/2003) and University Grant Commission, New Delhi for carrying out this research work.

References

1. Chou PT, MxMorrow D, Aartsma TJ (1984) J Phys Chem 88:4596–4599. doi:10.1021/j150664a032
2. Catalan J, Paz JL, Valle JCD, Kasha M (1997) J Phys Chem A 198:5284–5291. doi:10.1021/jp970551k
3. Keck J, Roessler M, Schroeder C, Stueber GJ, Waiblinger F, Stein M, Legourrierec D, Kramer HEA, Hoier H, Henkel S, Fischer P, Port H, Hirsch T, Tytz G, Hayoz P (1998) J Phys Chem B 102:6975–6985. doi:10.1021/jp9818380
4. Martinej ML, Cooper WC, Chou TT (1992) Chem Phys Lett 193:151–154. doi:10.1016/0009-2614(92)85699-B
5. Shynkar VV, Klymchenko AS, Kunzelmann C, Duportail G, Muller CD, Demchenko AP, Freyssinet J-M, Mely Y (2007) J Am Chem Soc 129:2187–2193. doi:10.1021/ja068008h
6. Weller A (1961) Prog React Kinet 1:187–214
7. Lahmani F, Zehnacker-Rentien A (1997) J Phys Chem A 101:6141–6147. doi:10.1021/jp9712516
8. Gormin D, Sytnik A, Kasha M (1997) J Phys Chem A 101:672–677. doi:10.1021/jp962019n
9. McGarry PF, Jockusch S, Fujiwara Y, Kaprinidis NA, Turro NJ (1997) J Phys Chem A 101:764–767. doi:10.1021/jp961382r
10. Guallar V, Moreno M, Lluch J, Amat-Guerri MF, Douhal A (1996) J Phys Chem 100:19789–19794. doi:10.1021/jp962026b
11. Keck J, Kramer HEA, Port H, Hirsch T, Fischer P, Rytz G (1996) J Phys Chem 100:14468–14475. doi:10.1021/jp961081h
12. Parsapour F, Kelley DF (1996) J Phys Chem 100:2791–2798. doi:10.1021/jp9520106
13. Tarkka RM, Jenekhe SA (1996) Chem Phys Lett 260:533–538. doi:10.1016/0009-2614(96)00910-4
14. Zhang H, van der Meulen P, Glasbeek M (1996) Chem Phys Lett 253:97–102. doi:10.1016/0009-2614(96)00213-8
15. Mitra S, Das R, Bhattacharyya SP, Mukherjee S (1997) J Phys Chem A 101:293–298. doi:10.1021/jp961555c
16. Yi PG, Liang YH, Cao CZ (2005) Chem Phys 315:297–302. doi:10.1016/j.chem phys.2005.04.046

17. Nagaoka S, Nagashima U (1990) J Phys Chem 94:1425–1431. doi:10.1021/j100367a042
18. Nagaoka S, Nagashima U (1989) Chem Phys 136:153–163. doi:10.1016/0301-0104(89)80043-6
19. Verner MV, Scheiner S (1995) J Phys Chem 99:642–649. doi:10.1021/j100002a031
20. Sobolewski AL, Domcke W (1994) Chem Phys 184:115–124. doi:10.1016/0301-0104(94)00091-3
21. Catalan J, Palomar J, De PJLG (1997) J Phys Chem A 101:7914–7921. doi:10.1021/jp971582i
22. Carlo GD, Mascolo N, Izzo AA, Capasso F (1999) Life Sci 65:337–353. doi:10.1016/S0024-3205(99)00120-4
23. Hollman PCH, Arts ICW (2000) J Sci Food Agric 80:1081–1093
24. Ahcrne SA, O'Brien NM (2002) Nutrition 18:75–81
25. Shahidi F, Wanasundara PKJPD (1992) Crit Rev Food Sci Nutr 32:67–103
26. Sarkar M, Sengupta PK (1991) Chem Phys Lett 179:68–72. doi:10.1016/0009-2614(91)90293-1
27. Pivovarenko VG, Tuganova AV, Klimchenko AS, Demchenko AP (1997) Cell Mol Biol Lett 2:355–364
28. Klymchenko AS, Demchenko AP (2002) Langmuir 18:5637–5639. doi:10.1021/la025760x
29. Bondar OP, Pivovarenko V, Rowe GES (1998) Biochim Biophys Acta 1369:119–130. doi:10.1016/S0005-2736(97)00218-6
30. Klymchenko A, Duportail G, Ozturk T, Pivovarenko V, Mily Y, Demchenko A (2002) Chem Biol 9:1199–1208. doi:10.1016/S1074-5521(02)00244-2
31. Shynkar VV, Klymchenko AS, Mely Y, Duportail G, Pivovarenko VG (2004) J Phys Chem B 108:18750–18755. doi:10.1021/jp0467189
32. Roshal AD, Grigorovich AV, Doroshenko AD, Pivovarenko VG, Demchenko AP (1999) J Photochem Photobiol A Chem 127:89–100. doi:10.1016/S1010-6030(99)00105-7
33. Poteau X, Saroja G, Spies C, Brown RG (2004) J Photochem Photobiol A Chem 162:431–439. doi:10.1016/S1010-6030(03)00429-5
34. Sengupta PK, Kasha M (1979) Chem Phys Lett 68:382–385. doi:10.1016/0009-2614(79)87221-8
35. Khan AU, Kasha M (1983) Proc Natl Acad Sci USA 80:1767–1770
36. Sytnik A, Gormin D, Kasha M (1994) Proc Natl Acad Sci USA 91:11968–11972
37. Catalan J, del Valle JC, Diaz C, Palomar J, De PJLG, Kasha M (1999) Int J Quantum Chem 72:421–438
38. Dennison SM, Guharay J, Sengupta PK (1999) Spectrochim Acta Part A 55A:1127–1132
39. Klymchenko AS, Duportail G, Mely Y, Demchenko AP (2003) Proc Natl Acad Sci USA 100:11219–11224. doi:10.1073/pnas.1934603100
40. Chou P-T, Chen Y-C, Yu W-S, Cheng Y-M (2001) Chem Phys Lett 340:89–97. doi:10.1016/S0009-2614(01)00399-2
41. McMorrow D, Kasha M (1984) Proc Natl Acad Sci USA 81:3375–3378
42. Strandjord AJG, Courtncy SH, Friedrich DM, Barbara PF (1983) J Phys Chem 87:1125–1133. doi:10.1021/j100230a008
43. Woolfe GJ, Thistlethwaite PJ (1981) J Am Chem Soc 103:6916–6923. doi:10.1021/ja00413a026
44. del Valle JC (2006) J Chem Phys 124:104506–104518. doi:10.1063/1.2177256
45. Falkovskaia, Pivovarenko VG, del Valle JC (2003) J Phys Chem A 107:3316–3325. doi:10.1021/jp021791p
46. Falkovskaia, Pivovarenko VG, del Valle JC (2002) Chem Phys Lett 352:415–420. doi:10.1016/S0009-2614(01)01490-7
47. De SP, Ash S, Bar HK, Bhui DK, Dalai S, Misra A (2007) Theochem 824:8–14. doi:10.1016/j.theochem.2007.08.014
48. Catalan J, del Valle JC, Palomer J, Diaz C, de Paz JLG (1999) J Phys Chem A 103:10921–10934. doi:10.1021/jp992631p
49. Bouchy A, Rinaldi D, Rivail JL (2004) Int J Quant Chem 96:273–281
50. Dreuw A, Head-Gordon M (2005) Chem Rev 105:4009–4037. doi:10.1021/cr0505627
51. Datta A, Mallajosyula SS, Pati SK (2007) Acc Chem Res 40:213–221. doi:10.1021/ar0682738
52. Becke AD (1993) J Chem Phys 98:5648–5652. doi:10.1063/1.464913; Lee C, Yang W, Parr RG (1988) Phys Rev B 37:785–789. doi:10.1103/Phys Rev B.37–785
53. Barone V, Adamo C (1995) J Phys Chem 99:15062–15068. doi:10.101/j100041a022
54. Frisch MJ, Trucks GW, Schlegel HB, Scuseria GE, Robb MA, Cheeseman JR, Montgomery JR, Jr, Vreven T, Kudin KN, Burant JC, Millam JM, Iyengar SS, Tomasi J, Barone V, Mennucci B, Cossi M, Scalmani G, Rega N, Petersson GA, Nakatsuji H, Hada M, Ehara M, Toyota K, Fukuda R, Hasegawa J, Ishida M, Nakajima T, Honda Y, Kitao O, Nakai H, Klene M, Li X, Knox JE, Hratchian HP, Cross JB, Adamo C, Jaramillo J, Gomperts R, Stratmann RE, Yazyev O, Austin AJ, Cammi R, Pomelli C, Ochterski JW, Ayala PY, Morokuma K, Voth GA, P. Salvador P, Dannenberg JJ, Zakrzewski VG, Dapprich S, Daniels AD, Strain MC, Farkas O, Malick DK, Rabuck AD, Raghavachari K, Foresman JB, Ortiz JV, Cui Q, Baboul AG, Clifford S, Cioslowski J, Stefanov BB, Liu G, Liashenko A, Piskorz P, Komaromi I, Martin RL, Fox DJ, Keith T, Al-Laham MA, Peng CY, Nanayakkara A, Challacombe M, Gill PMW, Johnson B, Chen W, Wong MW, Gonzalez C, Pople JA (2004) Gaussian 03, Revision C.02. Gaussian Inc, Wallingford, CT
55. Vener MV, Scheiner S (1995) J Phys Chem 99:642–649. doi:10.1021/j100002a031
56. Sobolewski AL, Domcke W (1998) Chem Phys 232:257–265. doi:10.1016/S0301-0104(98)00110-4
57. Maheshwari S, Chowdhury A, Sathyamurthy N, Mishra H, Tripathi HB, Panda M, Chandrasekhar J (1999) J Phys Chem A 103:6257–6262. doi:10.1021/jp9911999
58. De SP, Ash S, Dalai S, Misra A (2007) Theochem 807:33–41. doi:10.1016/j.theochem.2006.12.010
59. De SP, Ash S, Bar HK, Bhui DK, Sarkar P, Sahoo GP, Misra A (2009) Spectrochim Acta A 71:1728–1735. doi:10.1016/j.saa.2008.06.032
60. Hunsberger IM (1950) J Am Chem Soc 72:5626–5635. doi:10.1021/ja01168a074